Quantum critical point and ferromagnetic semiconducting behavior in p-type $FeAs_2$

Bing-Hua Lei and Yuhao Fu
Department of Physics and Astronomy, University of Missouri, Columbia, Missouri 65211-7010, USA

Zhenzhen Feng
Department of Physics and Astronomy, University of Missouri, Columbia, Missouri 65211-7010, USA
Key Laboratory of Materials Physics, Institute of Solid State Physics,
Chinese Academy of Sciences, Hefei 230031, China and
Science Island Branch of Graduate School, University of Science and Technology of China, Hefei 230026, China

David J. Singh*
Department of Physics and Astronomy, University of Missouri, Columbia, Missouri 65211-7010, USA and
Department of Chemistry, University of Missouri, Columbia, MO 65211, USA
(Dated: November 15, 2019)

We illustrate a novel approach based on itinerant magnetism for finding ferromagnetic semiconductors that can be gate tuned to study quantum critical points. We show that p-type $FeAs_2$ is an example. The complex non-parabolic band structure of this material leads to a ferromagnetic instability when doped, while at the same time allowing for a modest transport effective mass. This leads to an analogy between magnetic semiconductors and thermoelectric materials.

Ferromagnetic semiconductors are of long-standing interest due to potential applications in electronic devices that use both charge and spin degrees of freedom. However, the subject also presents exciting physics due to the contradictory requirements for a good ferromagnetic semiconductor. [1–4] Importantly, magnetic semiconductors, if the magnetic properties are gate tunable and high mobility can be obtained, are of strong interest from a scientific point of view. In particular, they may provide an ideal platform for developing understanding of quantum criticality. [5–8] This is because gate tuning of magnetic properties potentially offers a very clean, repeatable method for detailed mapping out of transport and other properties [9, 10] through a quantum critical transition. This differs from more conventional quantum critical magnetic materials, such as $Sr_3Ru_2O_7$, $ZrZn_2$, $NbFe_2$ and others, where tuning parameters include chemical alloying, magnetic field and pressure. [7, 8, 11–16] Materials exhibiting gate tunable quantum criticality would allow detailed study of properties with controlled variation of magnetic field, carrier concentration and temperature.

Traditional approaches for realizing magnetic semiconductors are incorporation of magnetic impurities into conventional non-magnetic semiconductors, exemplified by Mn doped GaAs, and doping of ferromagnetic insulators. [17–22] However, these approaches are not ideal for studying critical points. In particular, in semiconductors where magnetic impurities are incorporated the Curie temperature could be tuned to zero by controlling the carrier concentration, but in that case the disorder in the magnetic impurity distribution may lead to glassy behavior rather than a clean quantum critical point. In doped magnetic materials magnetic ordering is a property of the starting intrinsic material, and therefore the Curie temperature may not be tunable to zero as needed for realizing a quantum critical point, even though the magnetic order may be switchable in some cases. [23]

Here we focus on an alternative approach based on itinerant magnetism, related to Stoner theory. [24–26] The itinerant ferromagnetism that can arise within this approach is directly due to an instability of the electron gas, and therefore resides in the same states that are responsible for transport. As such, strong transport signatures of spin-fluctuations associated with the critical point may be expected, perhaps similar to ruthenates, such as $Sr_3Ru_2O_7$. [7] We demonstrate here that semiconducting $FeAs_2$ has the possibility of being a ferromagnetic semiconductor when doped p-type and that this will be realized through a quantum critical point as a function of carrier concentration. Importantly, $FeAs_2$ is a three dimensional (3D) diamagnetic semiconductor. [27, 28] The fact that it is diamagnetic means that even though it contains a magnetic element in its chemical formula, it does not contain preformed moments in its undoped state.

It is also interesting to note that from a chemical point of view there are some similarities between $FeAs_2$ and the Fe-based superconductors, in particular, both systems show densities of states around the Fermi level that are dominated by Fe d states, but with significant covalency between Fe and As, and both show significant itinerancy in their electronic and magnetic properties. They also show short enough Fe-Fe distances (in-plane Fe-Fe in the Fe-based superconductors, and Fe chains in $FeAs_2$) to allow metal-metal bonding, affecting the electronic structure. [29, 30]

Ferromagnetism occurs in the Stoner model when the quantity $N(E_F)I/2 \geq 1$, where $N(E_F)$ is the Fermi level electronic density of states on a per atom basis and I is an interaction parameter that is material dependent,

* singhdj@missouri.edu

but typically ∼1 eV for 3d transition metal elements, and the factor of two is for the two spins contributing to the density of states. [31]

In a 3D semiconductor, the density of states is $N(E_F) \sim m^* E_F^{1/2}$, with E_F relative to the band edge, while the mobility generally varies as $\mu \sim 1/m^*$. Additionally, the Curie temperature in itinerant models generally decreases with the energy scale, which is governed by $1/m^*$. [32] This leads to a conundrum if one seeks ferromagnetic semiconductors based on this approach – one seeks materials that have both a very heavy effective mass and at the same time a low effective mass. A related conundrum arises in thermoelectric materials, where high performance requires both high conductivity and high Seebeck coefficient, in other words light mass and heavy mass at the same time. In thermoelectrics this can be resolved through complex band structures. [33–37] These favorable band structures can lead to transport effective masses that are much lower than would be inferred from the Seebeck coefficient. We suppose then that thermoelectric materials may be a good starting point for finding ferromagnetic semiconductors.

$FeAs_2$ is a diamagnetic semiconductor occurring in the orthorhombic marcasite structure, [38] space group $Pnnm$ (#58). [27, 28, 39, 40] It has interesting thermoelectric properties when doped n-type, [27, 41] including high Seebeck coefficients at high carrier concentration, and a complex non-parabolic band structure. [42] Importantly, these properties are well described by standard density functional theory (DFT) calculations in Fe_2As. [42, 43] Here we use DFT calculations to investigate $FeAs_2$ as a ferromagnetic semiconductor.

We did calculations using the general potential linearized augmented planewave method, [44] implemented in the WIEN2k code, [45] with the standard PBE generalized gradient approximation (PBE GGA). [46] We tested different choices for the LAPW sphere radii. The results shown are for radii of 2.20 Bohr. We used well converged basis sets consisting of LAPW functions plus local orbitals, with a planewave sector cutoff of $R_{min}K_{max}$=9, and we crosschecked using the projector augmented wave (PAW) method as implemented in the VASP code, [47, 48] with an energy cutoff of 450 eV.

Fig. 1 shows the calculated electronic density of states (DOS), and band structure, which are similar to prior reports. [49] Near the band edges the DOS is mainly derived from Fe d states. As seen, for n-type values of the DOS significantly exceeding the Stoner criterion, roughly, $N(E_F)/2 = \geq 1$ eV^{-1} are not achievable. On the other hand, the valence band shows a prominent Fe d derived peak below the band edge, and the DOS onset is much steeper for p-type than for n-type. Interestingly, even though the high DOS indicates very heavy bands, there is significant dispersion of bands near the band edge reflecting the presence of multiple bands and non-parabolicity. The Stoner criterion, based on the DOS with I=1 eV applied to the Fe d component, is exceeded for E_F below ∼ -0.13 eV, relative to the valence band maximum, which is

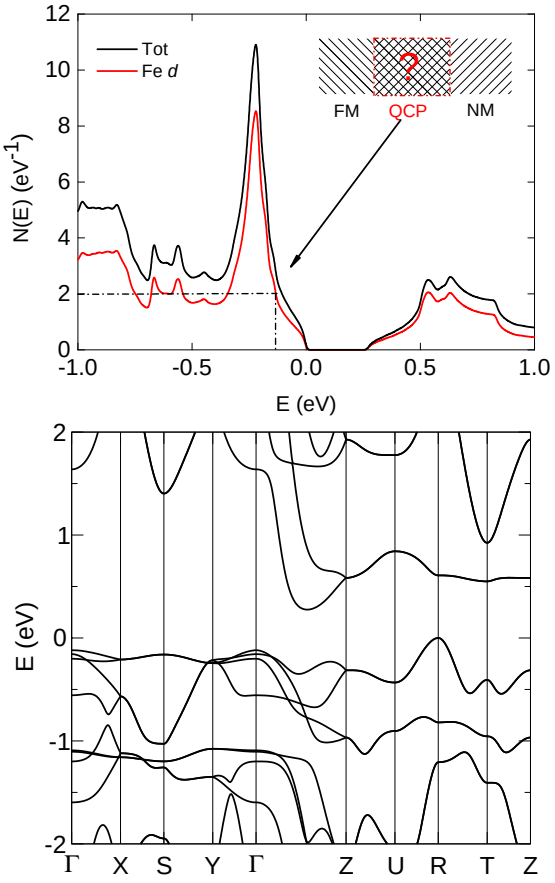

FIG. 1. Total and partial density states of $FeAs_2$ on a per formula unit both spins basis (top) and band structure (bottom). The energy zero is the valence band maximum. The point at which the Stoner criterion with I=1 eV for Fe is exceeded is indicated.

a value that may be reachable by gating and/or doping.

The first question is whether a ferromagnetic instability can be realized in p-type $FeAs_2$. We did virtual crystal calculations with constrained DFT employing the fixed spin moment procedure to investigate this. The virtual crystal approximation is a self-consistent average potential method that does not rely on rigid bands and is appropriate for gate tuning as well as doping provided that the potential due to the dopant atoms is not too strong. We also did calculations with explicit doping on the As site using replacement by Ge in a supercell of composition Fe_4GeAs_7. The results are given in Fig. 2.

As seen, itinerant ferromagnetism at the mean field level starts at low doping, $\sim x$=4%, where, x corresponds to substitution on the As site with an element providing one fewer valence electrons (thus the number of holes per Fe is $2x$). Also, the predicted magnetization is close to the maximum allowed by the doping level over a wide range, implying a high spin polarization. It is also noteworthy that the results for the explicit substitution on the As site are similar to the virtual crystal calculations. We also did self-consistent virtual crystal calculations in-

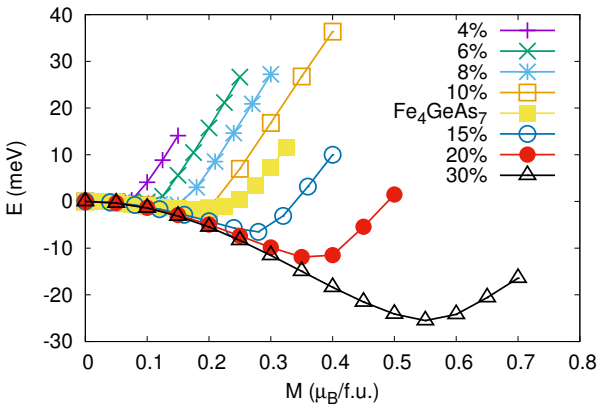

FIG. 2. Total energy $FeAs_2$ as a function of constrained spin magnetization on a per formula unit basis in the virtual crystal approximation. The energy of non-spin-polarized case was set to zero. The percent values are holes per As (corresponding to replacement of As by e.g. Ge. The results of an explicit Fe_4GeAs_7 supercell calculation corresponding to 12.5% are also shown.

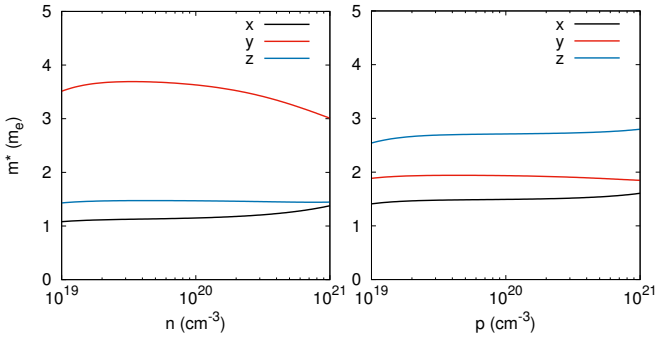

FIG. 3. Calculated direction dependent 300 K transport effective mass of n-type (left lines) and p-type (right lines) $FeAs_2$ function of carrier concentration.

cluding spin-orbit coupling. We find similar magnetic instabilities in that case.

However, as mentioned, a magnetic instability by itself is not sufficient to make a material a good ferromagnetic semiconductor, since transport is important. The band structure is shown in the bottom panel of Fig. 1 The band gap is indirect and has a value of 0.27 eV, consistent with reported experimental values of 0.22 eV and 0.24 eV, [27, 41] and a prior calculated value of 0.28 eV. [43] The agreement of the PBE value with experiment is perhaps surprising, but we note that this has been found in the past for materials where both the conduction band and valence bands are derived from d electrons and where correlation effects are not strong. This is because crystal field splittings are often well described by standard DFT calculations. [50]

There are flat bands near the valence band edge, which underlie the large peak in the DOS that causes the Stoner instability when doped p-type. Importantly, however,

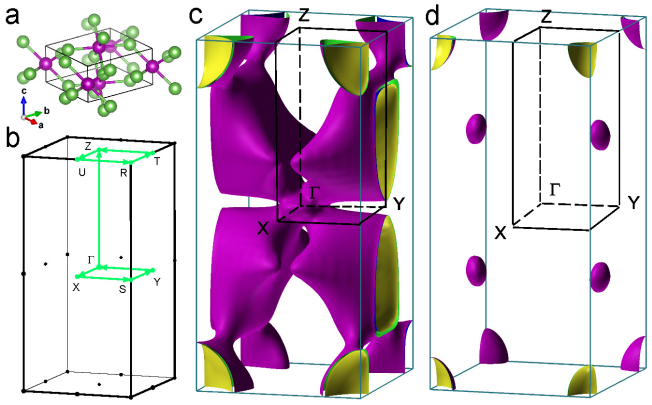

FIG. 4. The left panel shows (a) the crystal structure and the (b) Brillouin zone of $FeAs_2$. The middle and right panels show (c) minority and (d) majority spin Fermi surfaces of ferromagnetic $FeAs_2$ at 10% doping (0.2 holes per Fe).

there are also more dispersive bands, in particular at the R point valence band maximum, in the dispersion of the second and third bands from the band edge along Γ-Z and also along Γ-S. Therefore, in analogy with thermoelectric materials, this may be a case where the transport and density states are decoupled in the sense of not following the expectations of a parabolic band model.

We calculated the transport function, σ/τ (σ is conductivity, τ is relaxation time), using the BoltzTraP code, [51] in order to determine the transport effective mass. This is the effective mass that governs transport, and is defined as the carrier concentration and temperature dependent mass that would give a value of σ/τ in a parabolic band model that is the same as the actual value with the real band structure. [52] The results at 300 K are shown in Fig. 3 for both p-type and n-type. As seen, the transport effective mass is significantly anisotropic for n-type. This is due to anisotropic carrier pockets (not shown). The transport mass shows lower but still significant anisotropy for p-type, which is the subject of the present work, with the out-of-plane z (c-axis) direction mass being higher than the in-plane, x and y direction masses. Importantly, even though the near band edge DOS for $FeAs_2$ is very high, the material is a 3D semiconductor with an effective mass that is not so high as to preclude transport studies. It is also interesting to note that even though the onset of the DOS at the band edge is steeper for p-type than for n-type, the transport effective masses are comparable.

We now turn to the spin-polarization. The doped holes in this material are highly polarized as seen from the spin magnetization. Fig. 4 shows the minority and majority spin Fermi surfaces at doping level of 10% (0.2 holes per Fe). This corresponds to a carrier concentration of 4.35×10^{21} cm^{-3}. The calculated spin moment is 0.185 μ_B per formula unit. The minority spin shows hole Fermi surfaces located at the zone corner R point, where there are two relatively light bands (degenerate at

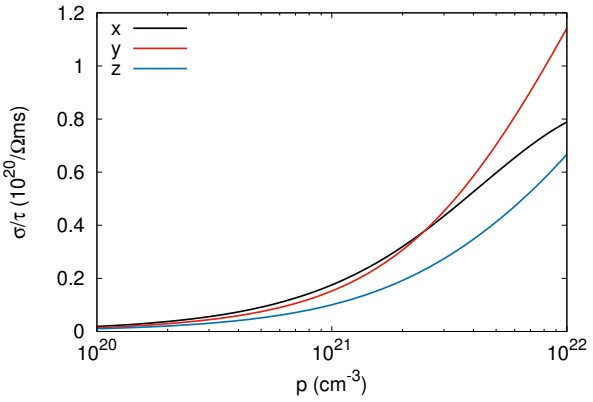

FIG. 5. σ/τ as a function of hole concentration at 300 K in p-type $FeAs_2$.

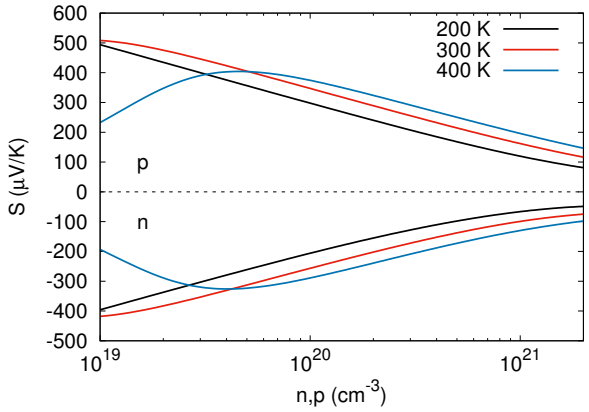

FIG. 6. Direction averaged Seebeck coefficient as a function of carrier concentration at 200, 300 and 400 K in $FeAs_2$.

R, Fig. 1) yielding two small surfaces and larger surfaces along the line between Y and T (around H), where there are two heavy bands degenerate along Y-T yielding larger hole Fermi surfaces with shapes that are distinctly different from ellipsoids, reflecting the non-parabolicity of the band structure. At 10% doping shown, these R and H surfaces touch forming necks. The majority spin surfaces are similarly located, but are small, as expected.

The spin polarization is $P_f = (f_\uparrow - f_\downarrow)/(f_\uparrow + f_\downarrow)$, for quantity f, which can be the conductivity σ, for the transport spin polarization, P_σ, or the density of states, $D = N(E_F)$, for the density of states spin polarization, P_D or other quantities. The charge spin polarization (the polarization of the doped carriers), P_c is 0.85. The DOS spin polarization, P_D=-0.83, is negative. This negative P_D simply reflects the fact that it is doped holes that are polarized. The transport spin polarization, P_σ, may be obtained from transport function, σ/τ, if the relaxation time, τ, is similar for the two spins, which is often a reasonable approximation. [53] We obtain direction dependent values, $P_{\sigma,x}$=-0.73, $P_{\sigma,y}$=-0.77, and $P_{\sigma,z}$=-0.79, calculated at 100 K using BoltzTraP. Thus both the transport and density of states spin polarization values are similar and both are negative. Thus, while not half-metallic in this doping range, p-type $FeAs_2$ does have a very high spin polarization both for diffusive transport, governed by P_σ, and tunneling, governed by P_D.

Returning to the semiconducting properties, Fig. 5 shows the direction dependent transport function σ/τ as a function of p-type carrier concentration at 300 K for non-spin polarized $FeAs_2$. The calculated direction averaged Seebeck coefficients, as obtained in the constant scattering time approximation are given in Fig. 6. Outside the bipolar regime (the regime at low doping and high T where $|S|$ increases with carrier concentration), S is reasonably isotropic, as is normal in semiconductors. [54] For comparison, state-of-the-art thermoelectrics such as Bi_2Te_3 and its alloy with Sb_2Te_3, show $|S|$ in the range $\sim$200–250 μV/K at ambient temperature and carrier concentrations of $\sim 10^{19}$ cm^{-3}. [55, 56] The numerical values of σ/τ as a function of carrier concentration will allow extraction of the scattering rate as a function of doping and temperature when experimental values become available. Consistent with the transport effective mass, σ/τ is highest in the plane of the a and b crystallographic directions (x-y plane). In this plane it is nearly isotropic up to hole concentrations of $\sim 2\times 10^{21}$ cm^{-3}, above which the y direction has significantly higher conductivity. The Seebeck coefficients are interestingly large even for high carrier concentration, with higher values for p-type than for n-type. The higher $|S|$ for p-type is consistent with the steeper onset of the DOS for p-type. Even at 300 K, and a carrier concentration of 10^{20} cm^{-3} a value $S(300)$ exceeding 300 μV/K is obtained. This suggests that p-type $FeAs_2$ is a material whose p-type thermoelectric performance should be experimentally investigated if high doping can be achieved.

To summarize, diamagnetic $FeAs_2$ can be made ferromagnetic by p-type carrier doping. This may be by gate tuning or potentially by chemical doping. In the case of gate tuning this may be a very interesting three dimensional material for study of quantum critical behavior. We note that organometallic chemical vapor deposition growth of $FeAs_2$ on GaAs has been demonstrated. [57]

In our mean field-like DFT calculations, we find ferromagnetism at modest carrier concentrations below 0.1 holes per Fe. In reality, this ferromagnetism will be renormalized by spin fluctuations associated with the critical point. Such spin fluctuations can be mapped out via transport measurements. Therefore it will be of considerable interest to study whether the critical point can be reached and if so at what carrier concentration it occurs. It will also be of interest to measure resistivity and field dependence to understand the evolution of spin fluctuations with carrier concentration and temperature.

In addition, the high Seebeck coefficients of $FeAs_2$ suggest measurements of the field dependence of the Seebeck coefficient. One possibility is that the Seebeck coefficient may show a suppression with field with near the critical point, analogous to the high susceptibility, high Seebeck

coefficient layered material, Na_xCoO_2, [58, 59] which would provide an interesting 3D analogue. Mapping out the field, carrier concentration and temperature dependence of the Seebeck coefficient near a quantum critical point may provide new insights into quantum criticality. In any case, the present work suggests investigation of p-type $FeAs_2$ as a material that may show a quantum critical point followed by ferromagnetic semiconducting behavior at higher carrier concentrations. Finally, while $FeAs_2$ presents an unusual situation, it is probably not unique. We hope that our work will stimulate further investigation of other materials leading to the discovery of other cases.

This work was supported by the U.S. Department of Energy, Basic Energy Sciences, Award DE-SC0019114.

[1] S. A. Wolf, Science **294**, 1488 (2001).
[2] I. Žutić, J. Fabian, and S. D. Sarma, Rev. Mod. Phys. **76**, 323 (2004).
[3] A. H. MacDonald, P. Schiffer, and N. Samarth, Nat. Mater. **4**, 195 (2005).
[4] K. Ando, Science **312**, 1883 (2006).
[5] J. A. Hertz, Phys. Rev. B **14**, 1165 (1976).
[6] P. Coleman and A. J. Schofield, Nature **433**, 226 (2005).
[7] S. A. Grigera, R. S. Perry, A. J. Schofield, M. Chiao, S. R. Julian, G. G. Lonzarich, S. I. Ikeda, Y. Maeno, A. J. Millis, and A. P. Mackenzie, Science **294**, 329 (2001).
[8] A. Steppke, R. Kuchler, S. Lausberg, E. Lengyel, L. Steinke, R. Borth, T. Luhman, C. Krellner, M. Nicklas, C. Geibel, F. Steglich, and M. Brando, Science **339**, 933 (2013).
[9] S. Wu, J. S. Ross, G. B. Liu, G. Aivazian, A. Jones, Z. Fei, W. Zhu, D. Xiao, W. Yao, D. Codgen, and X. Xu, Nature Physics **9**, 149 (2013).
[10] J. Zeng, X. He, S. J. Liang, E. Liu, Y. Sun, C. Pan, Y. Wang, T. Cao, X. Liu, C. Wang, L. Zhang, S. Yan, G. Su, Z. Wang, K. Watanabe, T. Taniguchi, D. J. Singh, L. Zhang, and F. Miao, Nano Lett. **18**, 7538 (2018).
[11] A. Subedi and D. J. Singh, Phys. Rev. B **81**, 024422 (2010).
[12] R. P. Smith, M. Sutherland, G. G. Lonzarich, S. S. Saxena, N. Kimura, S. Takashima, M. Nohara, and H. Takagi, Nature **455**, 1220 (2008).
[13] F. Bondino, E. Magnano, M. Malvestuto, F. Parmigiani, M. A. McGuire, A. S. Sefat, B. C. Sales, R. Jin, D. Mandrus, E. W. Plummer, D. J. Singh, and N. Mannella, Phys. Rev. Lett. **101**, 267001 (2008).
[14] M. Sutherland, R. P. Smith, N. Marcano, Y. Zou, S. E. Rowley, F. M. Grosche, N. Kimura, S. M. Hayden, S. Takashima, M. Nohara, and H. Takagi, Phys. Rev. B **85**, 035118 (2012).
[15] A. Alam and D. D. Johnson, Phys. Rev. Lett. **107**, 206401 (2011).
[16] S. N. Khan and D. D. Johnson, Phys. Rev. Lett. **112**, 156401 (2014).
[17] H. Ohno, A. Shen, F. Matsukura, A. Oiwa, A. Endo, S. Katsumoto, and Y. Iye, Appl. Phys. Lett. **69**, 363 (1996).
[18] T. Dietl, Nat. Mater. **9**, 965 (2010).
[19] K. Sato, L. Bergqvist, J. Kudrnovsky, P. H. Dederichs, O. Eriksson, I. Turek, B. Sanyal, G. Bouzerar, H. Katayama-Yoshida, V. A. Dinh, T. Fukushima, H. Kizaki, and R. Zeller, Rev. Mod. Phys. **82**, 1633 (2010).
[20] N. T. Tu, P. N. Hai, L. D. Anh, and M. Tanaka, Appl. Phys. Lett. **108**, 192401 (2016).
[21] A. Hirohata, H. Sukegawa, H. Yanagihara, I. Zutic, T. Seki, S. Mizukami, and R. Swaminathan, IEEE Trans. Magnetics **51**, 0800511 (2015).
[22] W. Chen, J. George, J. B. Varley, G.-M. Rignanese, and G. Hautier, npj Comput. Mater. **5**, 72 (2019).
[23] B. Huang, G. Clark, D. R. Klein, D. MacNeill, E. Navarro-Moratalla, K. L. Seyler, N. Wilson, M. A. McGuire, D. H. Cobden, X. Xiao, W. Yao, P. Jarillo-Herrero, and X. Xu, Nature Nanotechnology **13**, 544 (2018).
[24] E. C. Stoner, Proceedings of the Royal Society of London. Series A. Mathematical and Physical Sciences **169**, 339 (1939).
[25] O. K. Andersen, J. Madsen, U. K. Poulsen, O. Jepsen, and J. Kollár, Physica B **86-88**, 249 (1977).
[26] G. L. Krasko, Phys. Rev. B **36**, 8565 (1987).
[27] A. K. Fan, G. H. Rosenthal, H. L. McKinzie, and A. Wold, J. Solid State Chem. **5**, 136 (1972).
[28] J. Lehmann-Horn, R. Yong, D. Miljak, and T. Bastow, Solid State Nucl. Magn. Reson. **71**, 87 (2015).
[29] D. J. Singh and M. H. Du, Phys. Rev. Lett. **100**, 237003 (2008).
[30] K. Kuroki, S. Onari, R. Arita, H. Usui, Y. Tanaka, H. Kontani, and H. Aoki, Phys. Rev. Lett. **101**, 087004 (2008).
[31] J. F. Janak, Phys. Rev. B **16**, 255 (1977).
[32] H. Tasaki, Phys. Rev. Lett. **69**, 1608 (1992).
[33] X. Chen, D. Parker, and D. J. Singh, Sci. Rep. **3**, 3168 (2013).
[34] D. S. Parker, A. F. May, and D. J. Singh, Phys. Rev. Appl. **3**, 064003 (2015).
[35] G. Xing, J. Sun, K. P. Ong, X. Fan, W. Zheng, and D. J. Singh, APL Materials **4**, 053201 (2016).
[36] H. Usui and K. Kuroki, J. Appl. Phys. **121**, 165101 (2017).
[37] G. Xing, J. Sun, Y. Li, X. Fan, W. Zheng, and D. J. Singh, Phys. Rev. Materials **1**, 065405 (2017), erratum, Phys. Rev. Materials **1**, 079901 (2017).
[38] F. Hulliger, Nature **198**, 1081 (1963).
[39] H. Holseth, A. Kjekshus, A. F. Andresen, and W. B. Pearson, Acta Chem. Scand. **22**, 3284 (1968).
[40] E. H. Roseboom, Am. Mineral. **48**, 271 (1963).
[41] N. Takeshita, A. Iyo, S. Ishida, H. Eisaki, and Y. Yoshida, J. Phys. Conf. Ser. **950**, 042024 (2017).
[42] H. Usui, K. Suzuki, K. Kuroki, S. Nakano, K. Kudo, and M. Nohara, Phys. Rev. B **88**, 075140 (2013).
[43] J. M. Tomczak, K. Haule, T. Miyake, A. Georges, and G. Kotliar, Phys. Rev. B **82**, 085104 (2010).
[44] D. J. Singh and L. Nordstrom, *Planewaves Pseudopotentials and the LAPW Method, 2nd ed* (Springer, Berlin, 2006).
[45] P. Blaha, K. Schwarz, G. K. H. Madsen, D. Kvasnicka,

and J. Luitz, *WIEN2k, An Augmented Plane Wave + Local Orbitals Program for Calculating Crystal Properties* (K. Schwarz, Tech. Univ. Wien, Austria, 2001).
[46] J. P. Perdew, K. Burke, and M. Ernzerhof, Phys. Rev. Lett. **77**, 3865 (1996).
[47] G. Kresse and J. Hafner, Phys. Rev. B **47**, 558 (1993).
[48] G. Kresse and J. Furthmuller, Phys. Rev. B **54**, 11169 (1996).
[49] G. K. H. Madsen, A. Bentien, S. Johnsen, and B. B. Iversen, in *2006 25th International Conference on Thermoelectrics* (IEEE, 2006).
[50] L. F. Mattheiss, Phys. Rev. B **43**, 1863(R) (1991).
[51] G. K. H. Madsen and D. J. Singh, Comput. Phys. Commun. **175**, 67 (2006).
[52] Z. Ran, X. Wang, Y. Li, D. Yang, X. G. Zhao, K. Biswas, D. J. Singh, and L. Zhang, npj Comput. Mater. **4**, 14 (2018).
[53] B. Nadgorny, M. S. Osofsky, D. J. Singh, G. T. Woods, R. J. Soulen, M. K. Lee, S. D. Bu, and C. B. Eom, Appl. Phys. Lett. **82**, 427 (2003).
[54] P. Shahi, D. J. Singh, J. P. Sun, L. X. Zhao, G. F. Chen, Y. Y. Lv, J. Li, J. Q. Yan, D. G. Mandrus, and J. G. Cheng, Phys. Rev. X **8**, 021055 (2018).
[55] B. Poudel, Q. Hao, Y. Ma, Y. Lan, A. Minnich, B. Yu, X. Yan, D. Wang, A. Muto, D. Vashaee, X. Chen, J. Liu, M. S. Dresselhaus, G. Chen, and Z. Ren, Science **320**, 634 (2008).
[56] H. Shi, D. Parker, M. H. Du, and D. J. Singh, Phys. Rev. Appl. **3**, 014004 (2015).
[57] P. J. Walsh and N. Bottka, J. Electrochem. Soc. **131**, 444 (1984).
[58] H. J. Xiang and D. J. Singh, Phys. Rev. B **76**, 195111 (2007).
[59] Y. Wang, N. S. Rogado, R. J. Cava, and N. P. Ong, Nature **423**, 425 (2003).